Nanoscale Res Lett (2010) 5:344–352
DOI 10.1007/s11671-009-9486-4

NANO EXPRESS

Profile Prediction and Fabrication of Wet-Etched Gold Nanostructures for Localized Surface Plasmon Resonance

Xiaodong Zhou · Nan Zhang · Christina Tan

Received: 7 October 2009 / Accepted: 29 October 2009 / Published online: 13 November 2009

Abstract Dispersed nanosphere lithography can be employed to fabricate gold nanostructures for localized surface plasmon resonance, in which the gold film evaporated on the nanospheres is anisotropically dry etched to obtain gold nanostructures. This paper reports that by wet etching of the gold film, various kinds of gold nanostructures can be fabricated in a cost-effective way. The shape of the nanostructures is predicted by profile simulation, and the localized surface plasmon resonance spectrum is observed to be shifting its extinction peak with the etching time.

Keywords Localized surface plasmon resonance (LSPR) · Nanosphere lithography (NSL) · Nanofabrication · Plasmonics · Nanoparticles · Profile simulation

Introduction

Nanoparticles have revolutionized conventional sensing technologies by magnifying signals and introducing unprecedented functionalities such as cloaking, image distortion correction, surface-enhanced Raman spectroscopy (SERS), electrical conduction in nanocircuits, cancer therapy with photothermal effects [1], etc., and these nanoparticles can be metallic [2–9] or bimetallic nanoparticles [10] and nanowires [11, 12]. Localized surface plasmon resonance (LSPR) [2–4, 7–9], generated by the interaction between the incident light and conduction electrons in noble metal nanoparticles to detect the refractive index variation around the nanoparticles, is one of the typical applications. As an alternative of surface plasmon resonance (SPR), which is an optical phenomenon on noble metal film for detecting analytes in real-time based on ambient refractive index variations, LSPR employs noble metal nanoparticles to enhance the electromagnetic field, simplifies the measurement setup, and has demonstrated similarity and superiority on the detections of biomarkers, DNA, and low molecular proteins.

Dispersed nanosphere lithography (NSL) is one of the best candidates to fabricate identical gold nanoparticles on a large area of glass substrate for LSPR in a mass productive way [7–9], because in LSPR, each metal nanoparticle serves as a separate emission element and thus periodicity is not required as long as they are evenly distributed. In dispersed NSL, metal film is evaporated in one to several times at different directions onto the nanospheres dispersed on the substrate, and the gold is subsequently dry etched. Due to the shade effect of the nanospheres, metal nanostructures are left on the substrate after the removal the nanospheres. Dispersed NSL can be used to acquire numerous shapes of metal nanostructures for tuning the peak wavelength and sensitivity of LSPR signal; however, its dry etching process increases the cost of LSPR chip, and glass or gold might contaminate the chamber of the expensive etching equipment such as argon milling or inductively coupled plasma (ICP) machine. To circumvent this problem, this paper demonstrates the approach to predict and fabricate gold nanostructures for LSPR by wet etching.

During the gold wet etching with the potassium iodide (KI) solution, glass will not be etched and keep intact, this

Electronic supplementary material The online version of this article (doi:10.1007/s11671-009-9486-4) contains supplementary material, which is available to authorized users.

X. Zhou (✉) · N. Zhang · C. Tan
Institute of Materials Research and Engineering (IMRE), A*STAR (Agency for Science, Technology and Research), 3, Research Link, Singapore 117602, Singapore
e-mail: donna-zhou@imre.a-star.edu.sg

is another advantage over dry etching, because dry etching tends to leave some over-etched trenches on the glass substrate [8] which will introduce some scattering loss. We consider two kinds of nanospheres: wet etching endurable and unendurable nanospheres. For example, polystyrene nanospheres will become waxy in the gold etchant, cover the gold and stop its etching, thus they have to be removed prior to wet etching. On the other hand, silica nanospheres keep intact during the wet etching, but it is difficult to be removed after etching. This paper simulated the obtainable gold nanostructure profiles after wet etching for both kinds of nanosphere masks, thus the fabrication process is designable and controllable by simulations.

In our preliminary experiments, we demonstrate that for a glass substrate with a gold film obliquely evaporated on the silica nanospheres, different wet etching time varies the shape of the gold nanostructures and shifts the LSPR spectra accordingly. Because the 3D gold nanostructures after wet etching are mainly under the silica nanospheres and cannot be observed by scanning electron microscope (SEM) or atomic force microscope (AFM), the profiles of the nanostructures at different etching intervals are also simulated, and we find that the trend of this wavelength shift is predictable by profile simulation. We have carried out the wet etching experiments with polystyrene nanospheres without removing them. These nanospheres became waxy (Fig. S1 in supplementary material) during the etching and inhabited the gold etching. However, we have successfully removed the polystyrene nanospheres by heating at 350 °C for 90 min (Fig. S2 in supplementary material). The experiments of wet etching after removing the nanospheres are under investigation and will be reported in the future.

Simulation

Theory

The profile simulation of the gold nanostructure on a nanosphere after one or several times of gold evaporation has been reported [13, 14]. In dispersed NSL, either 2D or 3D gold nanostructure, i.e., the gold on the nanosphere detaches or attaches from the gold on the substrate, will be formed around a discrete nanosphere depending on the gold evaporation angle and thickness. The 2D nanostructure is always conformal, i.e., gold only deposits along the profile of the nanosphere, while the 3D nanostructure can either be conformal (Fig. 1a) or non-conformal (Fig. 1b). Gold nanostructure will be reduced during wet etching as drawn in Fig. 1c.

In our previous paper [13], for the convenience of calculating the profile of the nanostructure, four intertransformable coordinate systems are introduced: the original coordinate system x_o–y_o–z_o, where the gold is evaporated at the angles of θ and φ (Fig. 1a); the coordinate system x_φ–y_φ–z_φ (where $y_\varphi = y_o$) with $\varphi = 0$, $\theta \neq 0$ (Fig. 1a); the coordinate system x_θ–y_θ–z_θ (where $z_\theta = z_\varphi$) with $\varphi = 0$, $\theta = 0$ (Fig. 1d); and the coordinate system $x_{\varphi c}$–$y_{\varphi c}$–$z_{\varphi c}$ for non-conformal gold deposition (Fig. 1b), where the non-conformal angle θ_c is the angle between y_θ and $y_{\varphi c}$. θ_c can be positive or negative depending on the materials and evaporation conditions. When θ_c is negative, the non-conformal part forms an undercut instead of the extension in Fig. 1b.

According to Fig. 1d, the gold evaporated on the nanosphere has the shape as shown in the study by X. Zhou et al. [13]

$$x_\theta^2 + \frac{y_\theta^2}{\left(1+\frac{t}{r}\right)^2} + z_\theta^2 = r^2 \tag{1}$$

where t is the thickness of the gold, r is the radius of the nanosphere, and the coordinate system x_θ–y_θ–z_θ has the relationship with the original coordinate system x_o–y_o–z_o as

$$\begin{cases} x_\theta = x_o \cos\varphi\cos\theta + z_o \sin\varphi\cos\theta - y_o \sin\theta \\ y_\theta = x_o \cos\varphi\sin\theta + z_o \sin\varphi\sin\theta + y_o \cos\theta \\ z_\theta = -x_o \sin\varphi + z_o \cos\varphi \end{cases} \tag{2}$$

The areas fulfill $x_\theta^2 + z_\theta^2 < r^2$ have no gold evaporated on the glass substrate, while other areas of the substrate have a gold deposition thickness of $t \cos\theta$. For multiple gold evaporation, the gross thickness is summated along the direction of each evaporation.

For non-conformal evaporation, the non-conformal part in the $x_{\varphi c}$–$y_{\varphi c}$–$z_{\varphi c}$ coordinate system is [13]

$$(1-t)x_{\varphi c}^2 + A_0 z_{\varphi c}^2 - A_0 r^2 = 0 \tag{3}$$

where $A_0 = 1 - T\cos^2(\theta + \theta_c)$, $T = \left(\frac{2t_k}{r} + \frac{t_k^2}{r^2}\right) \Big/ \left(1+\frac{t_k}{r}\right)^2$, θ is the gold evaporation angle, θ_c is the non-conformal angle in Fig. 1b, and $x_{\varphi c}$, $y_{\varphi c}$, and $z_{\varphi c}$ can be calculated with

$$\begin{cases} x_{\varphi c} = x_o \cos\varphi\cos\theta_c + y_o \sin\theta_c + z_o \sin\varphi\cos\theta_c \\ y_{\varphi c} = -x_o \cos\varphi\sin\theta_c + y_o \cos\theta_c - z_o \sin\varphi\sin\theta_c \\ z_{\varphi c} = -x_o \sin\varphi + z_o \cos\varphi \end{cases} \tag{4}$$

We suppose the wet etching is isotropic that all points exposed to the etchant are etched by a thickness of te along the normal direction of each point. For a quadric

$$\begin{aligned} &a_{11}x^2 + a_{22}y^2 + a_{33}z^2 + 2a_{12}xy + 2a_{13}xz + 2a_{23}yz \\ &\quad + 2a_1x + 2a_2y + 2a_3z + a_4 = 0 \end{aligned} \tag{5}$$

where $a_{11}^2 + a_{22}^2 + a_{33}^2 + a_{12}^2 + a_{13}^2 + a_{23}^2 \neq 0$, the normal to the surface at a point $N_0(x_0, y_0, z_0)$ on this surface is [15]

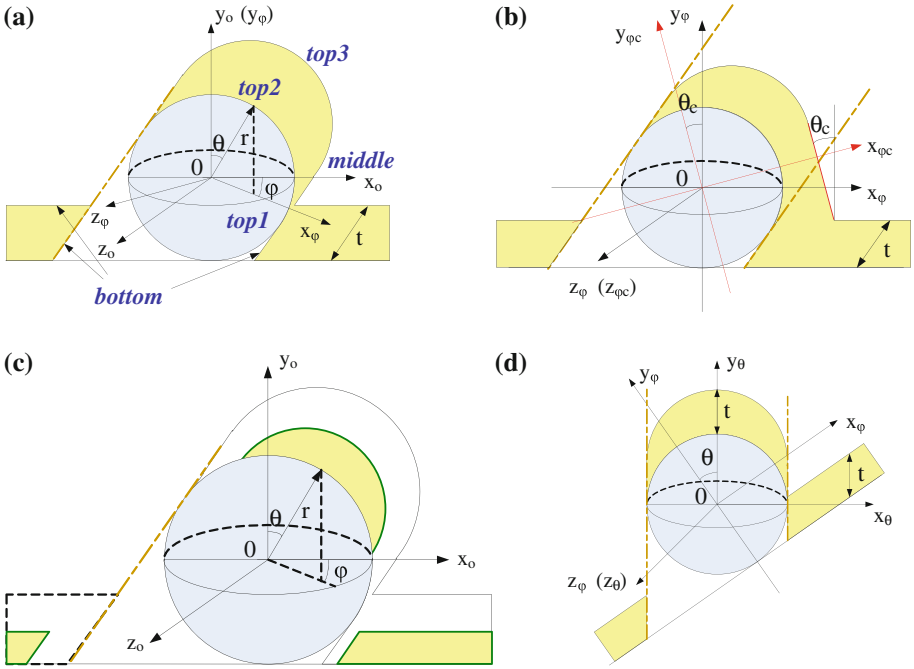

Fig. 1 Gold nanostructure around a nanosphere after oblique gold evaporation and wet etching. **a** shows 3D conformal gold nanostructure after gold evaporation; **b** is 3D non-conformal gold nanostructure when the angle θ_c is positive; **c** shows the nanostructure after wet etching; and **d** is for calculating the thickness of the gold after evaporation in the x_θ–y_θ–z_θ coordinate system, where the gold looks as if evaporated from the top of the nanosphere

$$\frac{x-x_0}{a_{11}x_0+a_{12}y_0+a_{13}z_0+a_1}=\frac{y-y_0}{a_{12}x_0+a_{22}y_0+a_{23}z_0+a_2}=\frac{z-z_0}{a_{13}x_0+a_{23}y_0+a_{33}z_0+a_3} \tag{6}$$

If the gold being etched is on the conformal part, based on Eq. 1, in the x_θ–y_θ–z_θ coordinate system, the normal to the surface at a point $P(x_\theta, y_\theta, z_\theta)$ is

$$\frac{1}{x_\theta}(x-x_\theta)=\frac{(1+t/r)^2}{y_\theta}(y-y_\theta)=\frac{1}{z_\theta}(z-z_\theta) \tag{7}$$

After wet etching, point P turns into a new point $P'(x_\theta', y_\theta', z_\theta')$ on the wet-etched surface, with the relationship of

$$\left(x_\theta-x_\theta'\right)^2+\left(y_\theta-y_\theta'\right)^2+\left(z_\theta-z_\theta'\right)^2=\mathrm{te}^2 \tag{8}$$

P' is also on the normal to the surface expressed by Eq. 7. Based on Eqs. 7 and 8, P' can be calculated by

$$\begin{cases} x_\theta'=x_\theta-\mathrm{te}\cdot x_\theta\Big/\sqrt{x_\theta^2+\dfrac{y_\theta^2}{(1+t_k/r)^4}+z_\theta^2} \\ y_\theta'=y_\theta-\mathrm{te}\cdot y_\theta\Big/\left((1+t_k/r)^2\sqrt{x_\theta^2+\dfrac{y_\theta^2}{(1+t_k/r)^4}+z_\theta^2}\right) \\ z_\theta'=z_\theta-\mathrm{te}\cdot z_\theta\Big/\sqrt{x_\theta^2+\dfrac{y_\theta^2}{(1+t_k/r)^4}+z_\theta^2} \end{cases} \tag{9}$$

If the gold being etched lies on the non-conformal part, by Eq. 3, in the $x_{\varphi c}$–$y_{\varphi c}$–$z_{\varphi c}$ coordinate system, the equation of the normal to this surface at the point $P(x_{\varphi c}, y_{\varphi c}, z_{\varphi c})$ is

$$\frac{x-x_{\varphi c}}{(1-t)x_{\varphi c}}=\frac{z-z_{\varphi c}}{A_0 z_{\varphi c}} \tag{10}$$

After wet etching, the new point $P'(x_{\varphi c}', y_{\varphi c}', z_{\varphi c}')$ is on the normal to the surface, it satisfies Eq. 10 as well as the condition

$$\left(x_{\varphi c}-x_{\varphi c}'\right)^2+\left(z_{\varphi c}-z_{\varphi c}'\right)^2=\mathrm{te}^2 \tag{11}$$

So $P'(x_{\varphi c}', y_{\varphi c}', z_{\varphi c}')$ is obtained by

$$\begin{cases} x_{\varphi c}'=x_{\varphi c}-\dfrac{(1-t)x_{\varphi c}\mathrm{te}}{\sqrt{(1-t)^2x_{\varphi c}^2+A_0^2z_{\varphi c}^2}} \\ z_{\varphi c}'=z_{\varphi c}-\dfrac{A_0z_{\varphi c}\mathrm{te}}{\sqrt{(1-t)^2x_{\varphi c}^2+A_0^2z_{\varphi c}^2}} \end{cases} \tag{12}$$

Since the calculated $P'(x_\theta', y_\theta', z_\theta')$ or $P'(x_{\varphi c}', y_{\varphi c}', z_{\varphi c}')$ can be converted back to the x_o–y_o–z_o coordinate system, Eqs. 9 and 12 form the profile of the gold nanostructure after wet etching.

Calculation Program

In order to simulate the nanostructure around a nanosphere after gold evaporation, five layers, namely, "bottom", "top1", "top2", "middle", and "top3" are calculated to form the whole complicated gold nanostructure [14], as indicated in Fig. 1a for conformal gold deposition and Fig. 2a for non-conformal gold deposition. They

respectively represent the gold on the substrate, on the lower and top parts of the nanosphere, and on the lower and top parts of the gold deposition outline. In the software, each layer is a data matrix, and they are drawn together to form the 3D profile of the gold nanostructure. After wet etching, five new layers "bottomwet", "top1wet", "top2-wet", "middlewet", and "top3wet" will be generated as plotted in Fig. 2b.

The simulation process is drawn in Fig. 3. First, the gold profile on the nanospheres with conformal gold deposition is calculated with Eq. 1; then the non-conformal part is calculated as a tangent cylindrical surface to the conformal part with Eq. 3; and finally the wet etching is calculated by Eq. 9 for the conformal part and Eq. 12 for the non-conformal part. Dry etching is calculated by reducing the etching thickness te from the "top3", "middle", and "bottom" layers. Dry etching is anisotropic where the etching is conducted directionally from top to bottom, while wet etching is isotropic that the dimension of the gold is reduced simultaneously from all directions. Thus, wet etching is more efficient and faster compared to dry etching.

The software is programmed with Fortran90. The output data from the 5 layers are plotted together in Mathcad to obtain the 3D profile of the gold nanostructure after gold deposition and after gold etching. They also can be plotted by other software such as Mathematica, Matlab, etc.

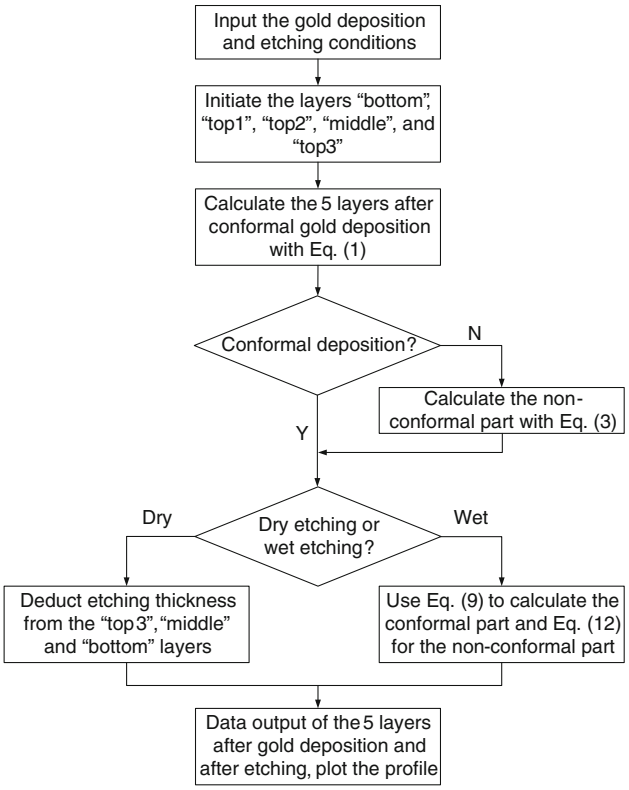

Fig. 3 Program process for calculating the gold nanostructure prior to and after gold etching

Simulation Examples

Wet etching can generate an abundance of various-shaped gold nanostructures. Figure 4 exemplifies that the profile of the nanostructure after gold evaporation is different for conformal and non-conformal gold nanostructures, as well as positive or negative non-conformal angles; and the nanostructure profile after different thickness of wet etching varies accordingly. For the conformal gold evaporation case in Fig. 4a–d, no gold protrudes on the substrate after wet etching, while for the non-conformal gold evaporations in Fig. 4e–l, the leftover gold nanostructure is much larger, some gold will remain on the substrate and form a cluster of gold nanoparticles around the silica nanosphere.

By comparing in pairs with Fig. 4c and d, or 4g and h, or 4k and l, it is found that the gold nanostructure obtained by keeping the nanosphere on and wet etching 30 nm of gold looks similar to the one obtained by removing the nanosphere and wet etching 15 nm of gold, because the former is single-side etching and the latter is double-side etching; but obviously the gold on the substrate is thicker for the latter one, as the gold on the substrate only experiences single-side etching. Since the gold is thick on the substrate due to three times of gold evaporation, gold remains on the substrate after 30 nm of wet etching.

Figure 5 compares the wet etching and dry etching of a gold nanostructure originally obtained with four times of gold evaporation, as presented in Fig. 5a. After wet etching 60 nm of gold with the nanosphere on the substrate, as shown in Fig. 5b, the gold on the nanosphere and some part on the substrate are etched away, and only 4 connected cones left around the nanosphere. When 30 nm of gold is

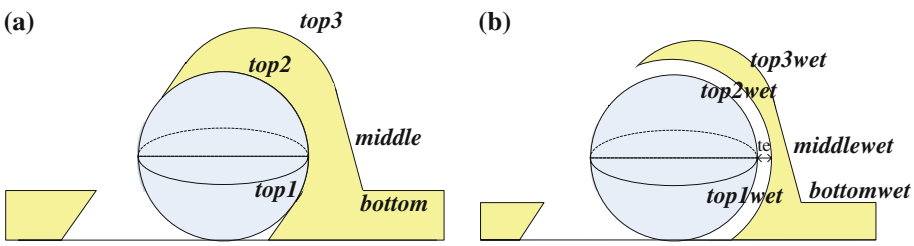

Fig. 2 Five profile layers for calculating the gold nanostructures **a** after gold deposition and **b** after wet etching. 3D non-conformal gold deposition is taken as an example. In **b**, it is assumed that the wet etching is conducted after removing the nanosphere

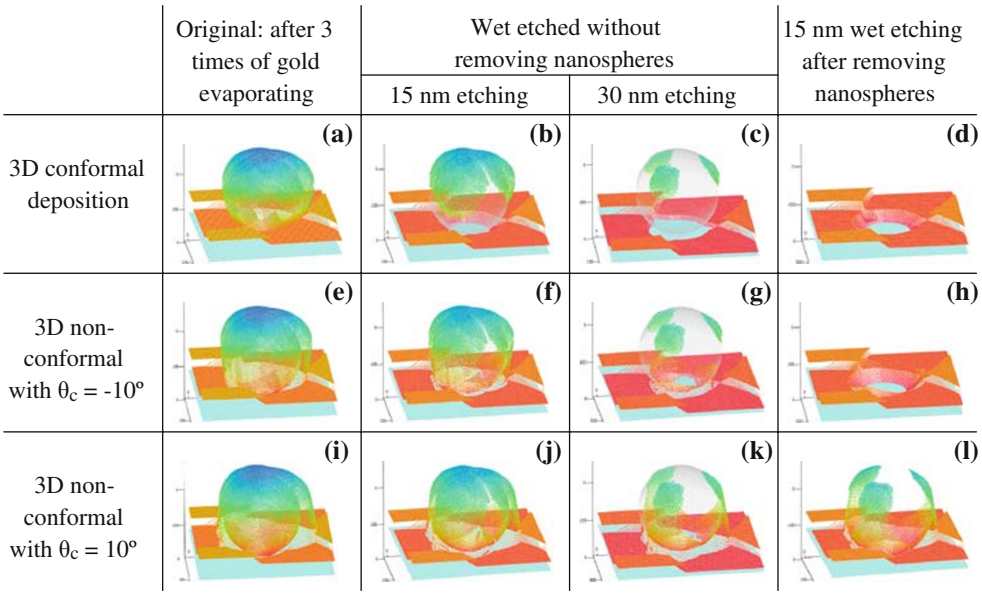

Fig. 4 Simulated profiles of the gold nanostructures after gold evaporation and wet etching. Before etching, 40 nm-thick gold film was evaporated 3 times at the angles of $\theta = 60°$, 60°, 60° and $\varphi = 0°$, 120°, 240° to the nanosphere. 3 kinds of gold depositions are simulated for wet etching: **a**–**d** are for 3D conformal gold deposition, **e**–**h** are for non-conformal gold deposition with $\theta_c = -10°$, and **i**–**l** are for non-conformal evaporation with $\theta_c = 10°$

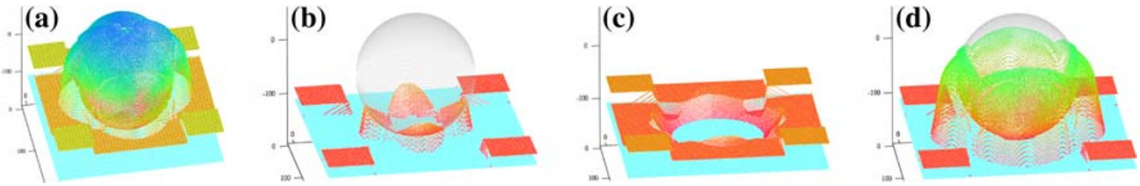

Fig. 5 Comparison for the profiles of the gold nanostructures obtained by wet etching and dry etching. **a** shows the nanostructure after evaporating 40 nm-thick gold film 4 times at the angles of $\theta = 60°$, 60°, 60°, 60° and $\varphi = 0°$, 90°, 180°, 270°, when the gold evaporations are non-conformal with $\theta_c = 10°$. **b** is after 60 nm of wet etching without removing the nanosphere, **c** is after 30 nm of wet etching after removing the nanosphere, and **d** is after 60 nm of anisotropic dry etching, assuming the nanosphere and the substrate are not etched during the dry etching

etched after removing the nanospheres, the etching is double side, but the leftover cones in Fig. 5c are about a half size of the ones in Fig. 5b. According to the results in Fig. 4k and l, the cones in Fig. 5b and c are expected to be in similar size. The prominent difference between Fig. 5b and c indicates that the profile of the wet-etched nanostructure is very sensitive to the gold deposition and etching conditions, thus the profile is hard to be roughly estimated but should be accurately simulated.

Figure 5d is with 60 nm of anisotropic dry etching. The leftover gold nanostructure on the nanosphere after 60 nm of dry etching is much larger than that of wet etching, because in dry etching the size of the nanostructure only reduces 60 nm from the top to bottom, while in wet etching, the 60 nm of gold is reduced in all directions; but the gold on the substrate is etched at the same depth for wet and dry etching, because in wet etching, one side of the gold on the substrate is protected by the substrate. In Fig. 5b and c, clusters of gold nanoparticles are left on the substrate, similar to those in Fig. 4. But in dry etching in Fig. 5d, clusters on the substrate are not generated. The clusters are interesting nanostructures in plasmonics, since it is reported that a dimer of nanoparticles emits much higher electrical field than a single nanoparticle [16], the narrow gaps between the clustered nanoparticles are expected to strongly enhance the plasmonic signal.

The simulations in Figs. 4 and 5 indicate that the size and shape of the gold nanostructure after wet etching are sensitive to the fabrication conditions such as the size of the nanosphere, gold evaporation angle and thickness, wet etching thickness, and whether the nanosphere is removed or not before etching. Because of these too many influential

factors, the profile simulation provides a useful tool to control the fabrication of the gold nanostructure by wet etching. We regard this simulation as important, also because the nanostructures after wet etching are hidden under unremovable silica nanospheres and are hard to be measured by SEM or AFM. Even the substrate can be tilt or cut to observe its side view in SEM, the 3D nanostructures cannot be fully inspected. On the other hand, the electrical charges in SEM are high when silica nanospheres and glass substrate are observed, the substrate has to be evaporated with a few nanometers of gold, and this layer of gold evaporation will deform the actual shape of the nanostructures. So in the following wet etching experiments, we simulated the wet-etched gold nanostructures to get their 3D shapes.

Experiments

Materials and Methods

In the experiments, silica nanospheres in the diameter of 175 nm were purchased from Microspheres-Nanospheres (a subsidiary of Corpuscular Inc.), and the silica nanospheres in the diameter of 500 nm were purchased from Duke Scientific Ltd. The chemicals poly(diallyldimethyl ammonium chloride) (PDDA), potassium iodide (KI), and iodide were from Sigma–Aldrich.

In order to disperse the silica nanospheres, a 4" Pyrex 7740 glass wafer was first implanted with silicon ions in Varian EHP-200 ion implanter at an energy of 5 keV and a dose of 1E14/cm^2 prior to being diced into 2 cm × 2 cm chips as substrates. After cleaning, the glass substrate was dip coated with a 1:5 diluted PDDA solution for 30 s; and after rinsing and drying, it was drop coated with 1 mL diluted nanosphere solution. The positive charges of PDDA canceled out the negative charges of the nanospheres as well as the charges of the implanted silicon ions on the glass substrate, thus the nanospheres were dispersed on the surface.

The silica nanospheres on the substrate were coated with gold film in R-Dec thermal evaporator, and then the sample was etched in the gold etchant formulated with 95% MilliQ water, 4% potassium iodide, and 1% iodide. In one of the experiments, the etchant was diluted 10 times to slow down the gold etching. The etching process was controlled both by LSPR spectra and SEM images at different etching intervals. The LSPR spectra were taken with Ocean Optics USB2000-UV–VIS optical fibre spectrometer at the wavelength range of 400–875 nm, and the dispersed nanospheres and wet-etched samples were inspected by JEOL JSM7400F field emission gun SEM.

Experimental Results

Shape of the Gold Nanostructures Versus Etching Time

To check the process of wet etching, 500 nm diameter silica nanospheres were deposited with 50 nm of gold at the angle of 70° and slowly wet etched at a 10 times diluted potassium iodide gold etchant. The oblique gold deposition angle is selected as 70°, because at 70°, 3D non-conformal gold nanostructure will be formed on 175 nm diameter nanospheres which are used in the experiment in Section "LSPR Spectra Variation Versus Etching Time". Because this experiment is to test the etching speed, we choose the same angle since the gold thickness on the substrate only depends on the gold evaporation angle. Before etching and after each 10 min of wet etching, the sample was rinsed and observed under SEM as shown in Fig. 6a–d. After 10 min of wet etching, the gold around the nanostructure and the substrate was thinner; after 20 min, only a little gold existed on the top of the nanosphere, and the gold film on the substrate was almost etched away; while after 30 min, no gold left on the substrate. Since the gold thickness on the substrate is 50 × cos (70°) = 17.1 nm, supposing the gold on the substrate was etched away after 20 min, the gold's etching rate for the 10 times diluted etchant is 0.855 nm/min. According to this etching rate, the side views of the nanostructures are simulated in the inserts

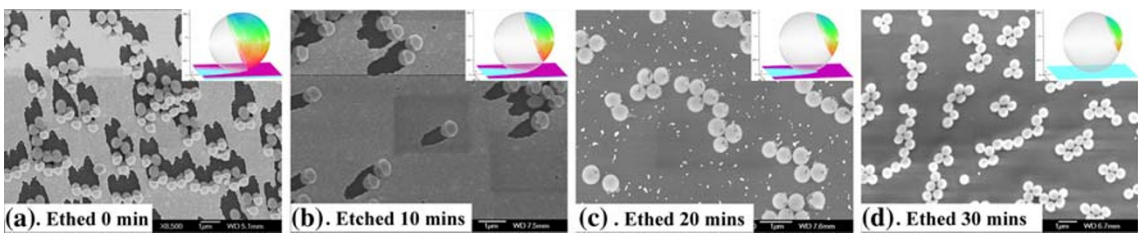

Fig. 6 The gold nanostructures **a** before, **b** during, and **c** and **d** after being etched in a 1:10 diluted potassium iodide gold etchant. Prior to etching, 50 nm of gold was evaporated onto 500 nm diameter silica nanospheres at 70°. *Scale bars* in SEM pictures are 1 μm. Inserts are simulated *side views* of the gold nanostructures

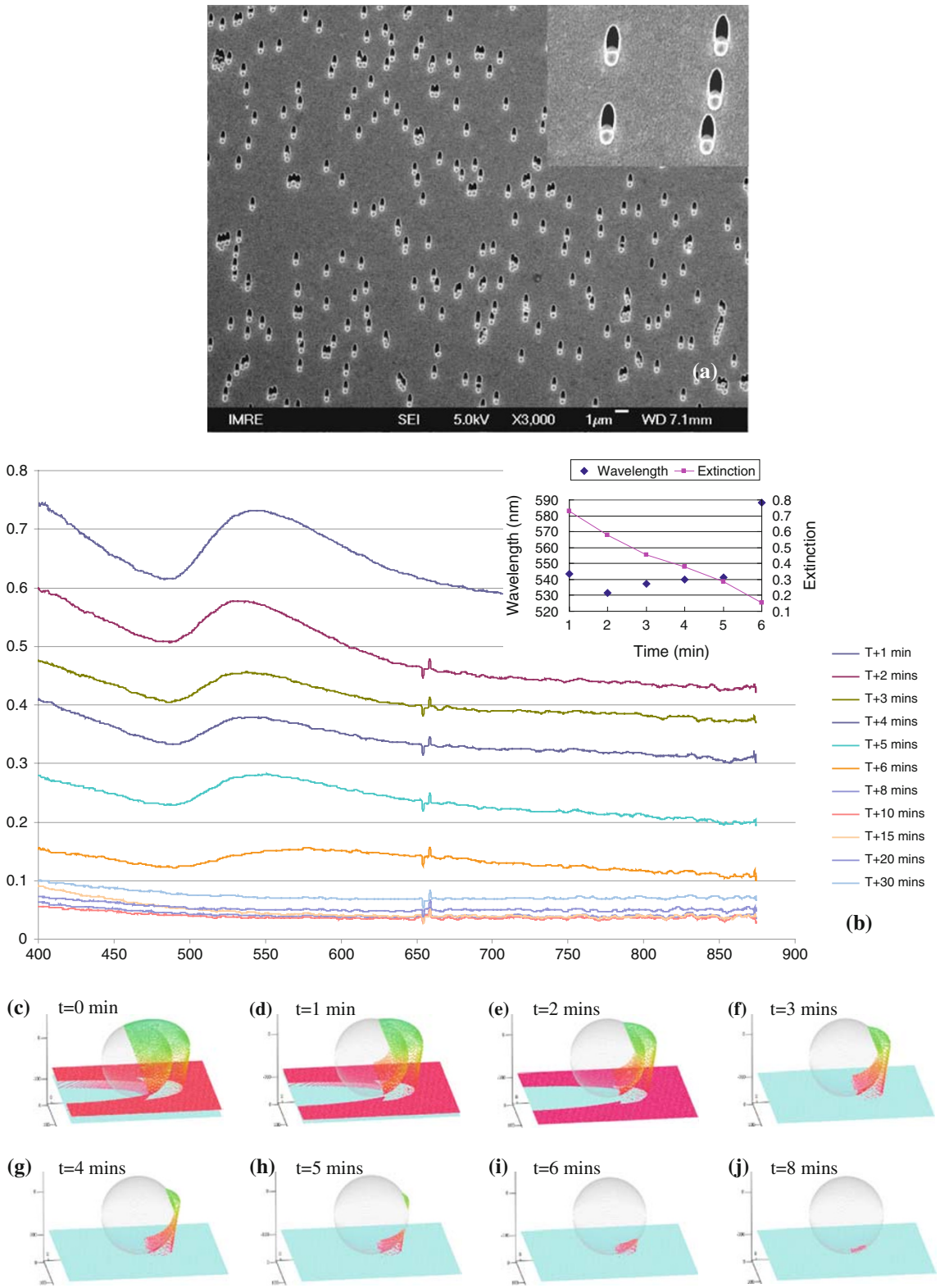

Fig. 7 Continuous wet etching of gold nanostructures in the undiluted etchant. **a** is SEM image of the sample before wet etching, which is obtained by evaporating 50 nm of gold onto the nanospheres of 175 nm in diameter at 70°, **b** shows the LSPR spectra of the sample after being wet etched for 1, 2, 3, 4, 5, 6, 8, 10, 15, 20, 30 min, **c**–**j** illustrate the shapes of the gold nanostructure before etching and after being etched 1, 2, 3, 4, 5, 6, and 8 min, respectively

of Fig. 6. The gold is thin compared with the 500 nm diameter of the nanospheres, so the gold nanostructure after gold evaporation is 2D, i.e., the gold on the nanosphere detaches from the gold on the substrate. As the undiluted gold etchant concentration is already low, the gold etching rate in the undiluted etchant is about 8.55 nm/min.

LSPR Spectra Variation Versus Etching Time

Another experiment was to wet etch the sample in an undiluted gold etchant and measure its LSPR spectra at different etching intervals to control the etching process. The silica nanospheres adhere to the glass substrate tightly due to the capillary force, they cannot be removed and their distribution does not change after etching, so the sample used to measure the LSPR spectrum was with the silica nanospheres on. The silica nanospheres in Fig. 6 were not well dispersed, by optimizing the concentration of the nanospheres by diluting it to a ratio of 1:15, better dispersion of silica nanospheres on glass substrate was achieved as shown in Fig. 7a, and this distribution is highly repeatable.

After evaporating 50 nm of gold onto the nanospheres of 175 nm in diameter at 70°, the obtained sample is as shown in Fig. 7a. The gold evaporation under this condition forms a 3D nanostructure around the nanosphere, based on the 3D formation condition $r \sin\theta + t\cos\theta > r$, where r is the radius of the nanosphere, θ is the gold deposition angle, and t is the gold evaporated thickness [13]. At the etching durations of 1, 2, 3, 4, 5, 6, 8, 10, 15, 20, 30 min, the sample was taken out, rinsed with DI water and dried for LSPR measurements, with the resultant spectra presented in Fig. 7b. The peak wavelengths of the LSPR spectra after 1–6 min of wet etching are, respectively, 543.4, 531.6, 537.5, 540.1, 541.4, and 588.2 nm, as plotted in the insert of Fig. 7b, and the LSPR peak disappeared after 8 min. Because it is difficult to inspect the gold nanostructures under SEM or AFM, we use some profile simulations to explain the trend of the LSPR shift.

Empirically, we know 3D gold nanostructure fabricated by gold evaporation is non-conformal with an angle θ_c. By fitting of the simulated profile, the possible gold nanostructures should have a non-conformal angle $\theta_c = -10°$. Because under this condition, after etching $8.55 \times 8 = 68.4$ nm of gold, only a little gold remains on the substrate as demonstrated in Fig. 7j, thus no LSPR spectrum is distinguishable. Taking $\theta_c = -10°$, we further simulated the nanostructure profiles after 0, 1, 2, 3, 4, 5, and 6 min of etching as illustrated in Fig. 7c–i. Comparing the size and shape variations of these nanostructures by time, the blueshift in the first 1–2 min was due to the quick size reduction [7, 9]; the peak wavelength kept almost unchanged at 3–5 min, because the reduced size of the nanostructure tended to blueshift the spectrum, while the reduced thickness to width ratio redshifted the spectrum [4, 7], two effects canceled out and did not exhibit obvious spectra shift; at 6 min, the LSPR spectrum redshifted a lot, because the thickness to width ratio of the nanostructures was greatly reduced when the gold on the nanosphere was etched away. This continuous peak tuning is an important feature for LSPR biosensing. In this experiment only 60 nm of LSPR wavelength shift was observed, because the original size of the silica nanospheres was only 175 nm. We expect to have larger LSPR wavelength shift range with larger silica nanospheres and thicker gold deposition.

As drawn in the insert of Fig. 7b, the extinction of the LSPR spectrum reduces with nanoparticle size reduction, because absorbance scales with the volume of the nanoparticle and scattering scales with the volume squared [17].

Conclusion

The fabrication of gold nanostructures through dispersed nanosphere lithography and wet etching was investigated. The profile simulation of wet-etched gold nanostructures under different fabrication conditions was carried out and could be used as a reference for parameter settings in fabrication process. In the preliminary experiments, we selected silica nanospheres as the mask as they endure gold etchant, we observed the LSPR spectrum of the wet-etched nanostructures shifted at different etching duration, correlated with the simulated profile of the nanostructures.

This wet etching method can acquire different kinds of gold nanostructures for LSPR sensing. Compared with dry etching conventionally used in dispersed NSL, wet etching is more cost-effective, it also reduces the optical scattering due to the rough glass surface caused by unspecific dry etching, and can form nanoparticle clusters that might further enhance the electromagnetic field of the nanostructures.

Acknowledgments We acknowledge Institute of Materials Research and Engineering (IMRE), A*STAR for its financial support of the project IMRE09/1C0420. We thank Miss Farhana Bibi Mahmud Munshi and Mr. Huei Ming Tan from National University of Singapore (NUS) for carrying out some wet etching experiments during their internship in IMRE, and Ms Sharon Oh in IMRE for beneficial discussions and help of taking some of the SEM images.

References

1. A.O. Govorov, W. Zhang, T. Skeini, H. Richardson, J. Lee, N.A. Kotov, Nanoscale Res. Lett. **1**, 84 (2006)
2. K.A. Willets, R.P. Van Duyne, Annu. Rev. Phys. Chem. **58**, 267 (2007)

3. J. Zhao, X. Zhang, C. Yonzon, A.J. Haes, R.P. Van Duyne, Nanomedicine **1**, 219 (2006)
4. C.R. Yonzon, E. Jeoung, S. Zou, G.C. Schatz, M. Mrksich, R.P. Van Duyne, J. Am. Chem. Soc. **126**, 12669 (2004)
5. G.L. Burygin, B.N. Khlebtsov, A.N. Shantrokha, L.A. Dykman, V.A. Bogatyrev, N.G. Khlebtsov, Nanoscale Res. Lett. **4**, 794 (2009)
6. J.B. You, X.W. Zhang, J.J. Dong, X.M. Song, Z.G. Yin, N.F. Chen, H. Yan, Nanoscale Res. Lett. **4**, 1121 (2009)
7. R. Bukasov, J.S. Shumaker-Parry, Nano Lett. **7**, 1113 (2007)
8. J.S. Shumaker-Parry, H. Rochholz, M. Kreiter, Adv. Mater. **17**, 2131 (2005)
9. H. Rochholz, N. Bocchio, M. Kreiter, New J. Phys. **9**, 53 (2007)
10. D. Mott, J. Luo, A. Smith, P.N. Njoki, L.Y. Wang, C.-J. Zhong, Nanoscale Res. Lett. **2**, 12 (2007)
11. J. Zhu, Nanoscale Res. Lett. **4**, 977 (2009)
12. H.H. Li, C.L. Liang, M. Liu, K. Zhong, Y.X. Tong, P. Liu, G.A. Hope, Nanoscale Res. Lett. **4**, 47 (2009)
13. X. Zhou, W. Knoll, K.Y. Liu, M.S. Tse, S.R. Oh, N. Zhang, J. Nanophotonics **2**, 023502 (2008)
14. X. Zhou, S. Virasawmy, W. Knoll, K.Y. Liu, M.S. Tse, L.W. Yen, Plasmonics **2**, 217 (2007)
15. A.D. Polyanin, A.V. Manzhirov, *Handbook of mathematics for engineers and scientists* (Chapman & Hall/CRC Press, Boca Raton, 2006)
16. S. Zou, G.C. Schatz, Chem. Phys. Lett. **403**, 62 (2005)
17. C.F. Bohren, D.R. Huffman, *Absorption and scattering by small particles* (Wiley, New York, 1983)